Nanoscale

Accepted Manuscript

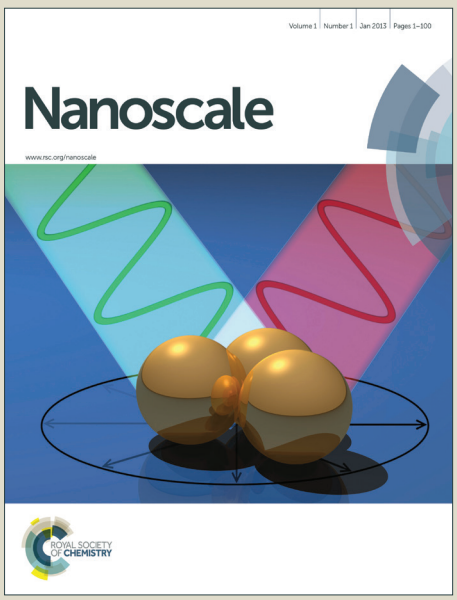

This is an *Accepted Manuscript*, which has been through the Royal Society of Chemistry peer review process and has been accepted for publication.

Accepted Manuscripts are published online shortly after acceptance, before technical editing, formatting and proof reading. Using this free service, authors can make their results available to the community, in citable form, before we publish the edited article. We will replace this *Accepted Manuscript* with the edited and formatted *Advance Article* as soon as it is available.

You can find more information about *Accepted Manuscripts* in the Information for Authors.

Please note that technical editing may introduce minor changes to the text and/or graphics, which may alter content. The journal's standard Terms & Conditions and the Ethical guidelines still apply. In no event shall the Royal Society of Chemistry be held responsible for any errors or omissions in this *Accepted Manuscript* or any consequences arising from the use of any information it contains.

ROYAL SOCIETY OF CHEMISTRY

www.rsc.org/nanoscale

Nanoscale

RSCPublishing

COMMUNICATION

Vortical superlattices in gold nanorods self-assembly monolayer

Cite this: DOI: 10.1039/xoxxoooooox

Yong Xie[a], Yujia Liang[a, d], Dongxue Chen[a, d], Xiaochun Wu[b], Luru Dai[c] and Qian Liu*[a]

Received ooth January 2012,
Accepted ooth January 2012

DOI: 10.1039/xoxxoooooox

www.rsc.org/

This paper describe novel vortical self-assembly of CTAB-capped gold nanorods. Representative left-hand, radial, and right-hand vortices are shown. Micelles formed by CTAB molecules enhance the organized self-assembly process. Drag force of solvent flow and dynamic vortex flow in the thin solvent layer have been thought to be responsible for the final vortical superlattices. FDTD simulation suggests these structures have potential properties in nanofocusing and polarized light response.

1. Introduction

Diverse microstructures made by inorganic nanocrystals emerge constantly over the past years[1-3]. These microstructures have been demonstrated their importance due to their collective optical, electronic, and plasmonic properties, as well as many other important applications[3]. However, up to now, tremendous efforts have been focused on the development of large-area, 2-dimensional or 3-dimensional self-assembly superlattices[4-7]. Few study deals with localized-area but distinctive structures in the general self-assemblies. Vortical superlattices are one of the interesting microstructures, and they have been continuously observed in many self-assembly processes. For example, vortexes were found in assembly of Tobacco Mosaic Virus[8], vortexes around singularities were found in $BaCrO_4$ nanorods assembly[9], CdSe nanorods with disclination strength of +1 were observed under a polarizing optical microscope[10] and transmission electron microscope[11], also, swirling cluster was also observed in gold nanorods self-assembly[12], and so on[13, 14]. In this paper, we focus on the vortical self-assembly superlattices formed by gold nanorods. Three kinds of new vortical morphologies are observed, they are left-hand, radial, and right-hand vortical superlattice, respectively. The formation mechanism of these vortices is clarified based on dynamic microscopic flow processes. The vortical results may suggest a likely strategy based on the liquid crystal template[5,6] or the microfluidic droplet to form and control the morphology of the ultimate self-assembled superstructure. In addition, potential optical properties of the vortical assemblies are simulated using 3-dimensional finite-difference time-domain (FDTD) approach, and nanofocusing and polarized light response are discussed.

2. Experimental section

A. Synthesis of gold nanorods

GNRs were synthesized according to modified seed-mediated growth method[I5]. The nanorods with the narrowest size-distribution (length of 59.5 ± 6.7, diameter of 17.0 ± 1.8 and aspect ratio of 3.5 ± 0.4) were used. The as-prepared GNRs were stabilized by surfactant cetyltrimethylammonium bromide (CTAB) in aqueous dispersion.

B. Preparation of vortical superlattices

Carbon-coated copper grid and silicon wafer were used as the substrates. 260 mesh carbon-coated copper grids were first fixed by lab-used vacuum belt onto the clean silicon wafers. 15 μL of the concentrated GNRs solution under the most optimized self-assembly condition of the GNRs concentration of ~33 nM and the CTAB concentration of ~2.5 mM[7,16], was pipetted onto the silicon wafer to cover the carbon-coated copper grids completely. The aqueous solvent was evaporated using an artificial climate chamber (STIK, CTHI-150B2) to guarantee a stable and controllable temperature and humidity. Drying of the colloidal solution led to the formation of the GNRs assemblies on the grids. The grids were finally detached from the silicon wafers and observed by transmission electron microscopy (TEM).

C. Sample characterization

Nanoscale Accepted Manuscript

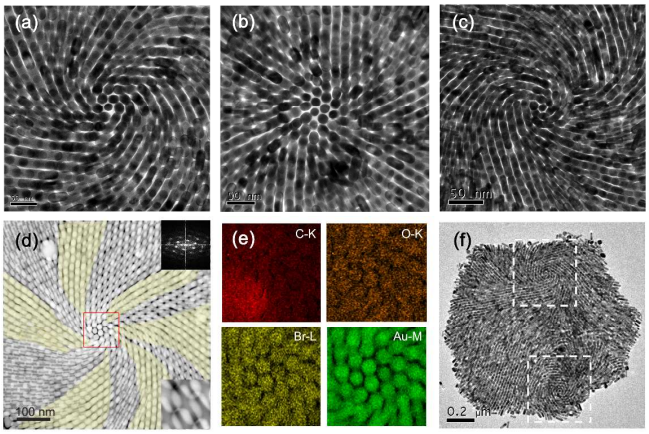

Fig. 1 TEM and EDX characterizations of the vortical superlattices (a)-(c) TEM images of left-hand, radial, and right-hand vortices, respectively. (d) Scanning TEM image with the highest contrast showed further details about the vortex, the insets are fast Fourier transform image (upper right) and smectic arrays (lower right), respectively. (e) EDX mappings of elements carbon, oxygen, bromine, and gold. (f) TEM image of mirrored twin-vortice superlattice.

TEM, Scanning-TEM and energy-dispersive X-ray analysis (EDX) were performed on Tecnai F20 U-TWIN and Tecnai T20 S-TWIN microscopes. SEM was performed on Hitachi S-4800 microscope. Optical properties were examined by FDTD simulation with an absorption boundary condition. The wavelength of incident light used was 500 nm close to the transverse absorption band of the nanorods (about 512 nm), the relative permittivity of the gold nanorod used was -2.55 + 3.37j. The vortical structure layout was built according to the actual structures: a central rod stood 90^o perpendicular to the substrate, the nearest-neighbour rods tilted 5^o respectively along the tangential direction, the next-nearest-neighbour rods tilted 10^o, and so forth. The vortical models were composed of 61 nanorods with length of 64 nm, diameter of 21 nm and separation of 3 nm. The incident light was radially-polarized and circularly-polarized wave, respectively.

3. Results and discussion

Fig. 1 shows the vortical superlattices of the GNRs. Right-hand (Fig. 1(a)) and left-hand (Fig. 1(c)) structures are presented for the first time, reflecting the potentially chiral feature of the localized self-assemblies. Fig. 1(b) shows the result of the self-assembly with a distinguishable centre despite without an obvious rotational feature. Such morphology is regarded as a transitional vortical superlattice, and termed as radial vortex. The three patterns represent the basic self-assembly vortices observed in the TEM samples, which were prepared by a controlled droplet evaporation method[7]. In order to make clear the structural characteristics of the vortex, we carried out high-contrast scanning TEM experiments as shown in Fig. 1(d). It can be seen clearly that the vortex is composed of two sets of different structures. In the yellow area the structures are mainly the nematic assembly of the GNRs[17], where the rods aligned end-to-end and eclipsed with each other. As a contrast, the rest area in the vortex showed mainly the smectic assembly of GNRs, where the rods aligned like crystals, and eclipsed with their nearby four rods as shown bottom inset in Fig. 1(d), where the bright areas are the eclipsed parts. Such a lattice structure forms spontaneously ordered nanoscale porosity, in which pore size is about 7 nm smaller than the synthetic limits of metallic mesoporous materials[18]. From the Fourier transform of the whole vortex area, the superlattice presents a hexagonal symmetry (Fig. 1(d), top inset), suggesting that the organised self-assembly structure should be formed in the solution prior to the formation of vortical morphologies on the carbon thin-film, because the hexagonal alignment in the CTAB-capped nanorods self-assemblies is the most stable structure[17,19,20]. The role of CTAB here supplies mainly the driving forces for the close-packed self-assembly. Specifically, CTA^+ bilayer capped on the GNRs surface by electrostatic interaction guarantees the enough repulsive force against the van der Waals attraction among the rods. Thus, the as-prepared GNRs are dispersed in the aqueous solution. With the evaporation of the droplet during the preparation process of the superlattices, both GNRs concentration and CTAB concentration are raised gradually, and eventually reach the critical concentration of the organised self-assembly process. Because CTAB micelles formed on a high CTAB concentration will produce additional depletion attraction, which breaks the balance between electrostatic force and van der Waals force, and finally induces and enhances the self-assembly process. Such a process has been confirmed by UV-vis absorption spectrum as reported in our work previously[7], where the assembly occurs obviously when CTAB concentration reaches higher than 0.4 M, and the assembly process intensifies gradually with the increase of the CTAB concentration. The self-assembly condition here is as same as the previous conditions. The large-area self-assembly of GNRs monolayer on the TEM grid is therefore formed during such a process. Figure 1(e) further shows the elemental composition of the self-assembled vortex obtained by EDX measurement. The elements of C, O, and Br disperse evenly in the surface of element Au, indicating there is an isolation layer of the stabilizer CTAB among the rods, and also suggesting that the CTAB is important in the self-assembly process. The separation between the bare GNRs is measured about 3 nm on average. Figure 1(f) shows that two mirrored vortices can be formed simultaneously in one assembly area, reflecting the interplay between the adjacent vortices in their formation process. From the dashed boxes, a full vortex has area of about 0.25 μm^2 generally. The effect of substrates on the vortices is also investigated, the results show that the vortices can be obtained also on the silicon surface, not only on the carbon film, as shown in Fig. 2(a).

To understand the mechanism underlying the formation of the vortex, more experimental results are provided as shown in Fig. 2. The previous reports often attributed the similar structures to the disclination of strength +1 or +1/2 in a nematic liquid-crystalline phase[9-11]. This can be supported partially in our experiments as shown in Figs. 2(b) and 2(c). Nonetheless, the origin of the vortices with mirrored feature cannot be explained from that viewpoint, here we propose a new explanation from a point of microscope flow. Local flows inside the solvent are often induced by spatially nonuniform temperature gradient, local concentrations, or unsymmetrical regions over the gird. As the solvent layer become thin during the droplet drying process, intensity of the microflows would become significant on the bottom of the droplet[21,22]. Considering this reason and the weak interactions between the GNRs and substrate, the forces produced by the microflows can be enough to change the morphology of the self-assemblies. As shown in Fig. 2(d) and Fig. 1(f), the observed mirrored twin-vortice superlattices are a typical evidence of this explanation. Furthermore, the self-assembly of the GNRs is affected by two main factors. One is Stokes dray force produced by the solvent microflows, which drags the sub-stable GNRs moving along the flows. Another is the vortical flow produced by inhomogeneity of the flow velocity. Especially, considering a central flow moves faster than its two side flows, a

Nanoscale Accepted Manuscript

 This journal is © The Royal Society of Chemistry 2012

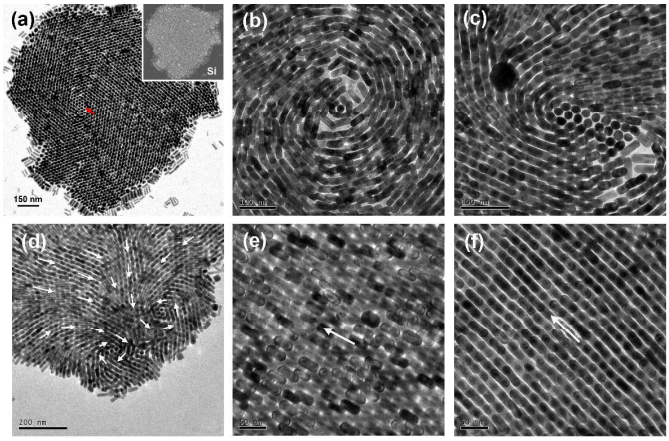

Fig. 2 (a) Vortical superlattice observed on silicon substrate. The image was changed by anti-color processing for improving the contrast. The arrow points out the position of the vortical center. The inset shows the raw SEM image on the silicon substrate. (b) and (c) TEM images for vortices with mentioned disclinations of strength +1 and +1/2. (d) Twin-vortices and the probable traces of flow lines, marked by arrows. (e) and (f) smectic and nematic arrays and the probable traces of flow lines.

spontaneous vortical flow can form in both side of the central flow when reaching a free end[13] or meet a barrier. Under the action of the flow field, the vortical superlattices are induced to form. In addition, the flow field can be formed in several patterns, therefore, it rationalizes diverse vortical superlattices as observed in Figs. 1 and 2. Here, it should be mentioned that the radial vortex and the concentric vortex (Fig. 1(b) and Fig. 2(b)) are found to be observed rarely, the cause may be that the relatively symmetric vortex flows or absolutely static flow in the solution are hard to form even in a near equilibrium environment. Also, due to random distribution of the flow fields and various defects, the morphology and formation position of the vortices are also random and appear with an equal probability or chance. Besides the vortex superlattices, Figs. 2(e) and 2(f) also show the obtained superlattices with different orientations and arranging modes (smectic in Fig. 2(e), nematic in Fig. 2(f)), which reflect the effect of probable unidirectional microflows in the evaporating droplet and support further our explanation of the microflow mechanism.

The spatial electromagnetic field intensity enhanced by surface plasmon effect of the vortex were analysed by FDTD simulation. Radially polarized light and circularly polarized lights were used to excite the optical response[23, 24]. A calculation model taking monolayer vortex as an example is shown in Fig. 3(a), where light propagates from top to bottom and the origin of coordinates (z=0) locates in the centre of central rod. Simulation results under an illumination of right-hand, radially and left-hand polarized light are shown in Figs 3(b)-3(j), respectively. It is easily seen that from Figs. 3(b)-3(d), the structural feature response at z=0 corresponding to the illumination of radially-polarized light is the most obvious. More interestingly, the spatial field intensity at z=-40 nm below the model bottom of 8 nm appears some hot spots similar to 'light needles' as shown in Figs. 3(e)-3(g). For the radially polarized light illumination, each rod's site produces a focused spot and the closer to the structure centre the stronger the light intensity, that is, the energy is concentrated gradually from the edge to the centre, showing a hierarchical, nanoscale focusing effect. The effect may originate from the constructive interference of the excited surface plasmon along the rods surface when they pass through the vortex. According to the literature[25-27], such a feature maybe useful in detecting or diagnosing certain small biological units, even in treating skin lesions using the localized heating effect. For the circular polarization incidence, as shown in Figs. 3(e) and 3(g), the field intensity at the edge of the vortical structures is enhanced obviously and presents a stationary handedness, i.e., left-hand property in Fig. 3(e) and right-hand property in Fig. 3(g), indicating that the vortices are responsive to the illumination of different circular polarized lights. The cause should be due to the constructive interference and the edge effect[28]. The asymmetry of the intensity distributions between Fig. 3e and Fig. 3g may result from the asymmetry of the studied model itself. As a comparative model, the field intensity of a left-hand vortex model can be exactly reflectional symmetry with the aforesaid right-hand vortex model. It should be noted that the field enhancement is not very strong due to too small vortical structure size (only sub-micron in diameter), but we believe that larger vortex would have larger field enhancement although we cannot yet obtain the larger vertex so far. For certifying this prediction, a larger model composed of 217 nanorods was built for further simulation. Figures 3(h)-3(j) shows the simulated results for the larger vortical model, where the size of the vortical model is twice than the initial model, the focusing effect shown in Fig. 3(i) is obviously increased as expected, and the same expectation is also verified in the handedness response on the edges shown in Figs. 3(h) and 3(j). These should originate from the average effect of multiple superposition and

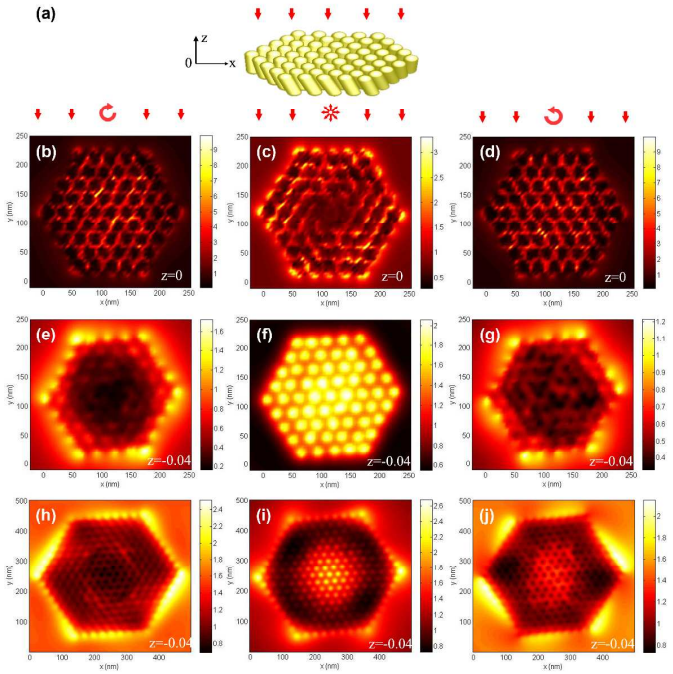

Fig. 3 FDTD simulation on optical properties of the GNRs vortices. (a) Calculated model of a right-hand vortex illuminated by different polarized lights from top to bottom. The origin of coordinates locates in the centre of central rod with length of 64 nm and diameter of 21 nm. The incident lights are right-hand, radial and left-hand polarized light, respectively. The corresponding results are shown from left to right. (b)-(d) Simulated distribution of intensity in the x-y plane at position z=0 nm on the model. (e)-(g) Simulated distribution of intensity at position z=-40 nm apart from the model bottom of 8 nm.

Nanoscale Accepted Manuscript

(h)-(j) Simulated distribution of intensity at position z=-40 nm based on a model with twice size.

interference of the incident light. It is concluded that if the size of actual vortical superlattices can be further increased by self-assembly experiment, the interesting vortical assembly structures will not only be able to solve practical problem, but also can realize various characterizations of optical property.

4. Conclusions

The vortical GNRs superlattices with left-hand, radial, and right-hand feature were assembled successfully and characterized by TEM, STEM and EDX. Arrays with alternative nematic and smectic phases were found in the superlattices. Upon analyzed the formation mechanism, we proposed that the drag force induced by solvent flow and the spontaneous vortex flow in the solution are the main causes for the formation of the vortical superlattices, implying that the microfluidic droplet may be a feasible strategy to form and control the morphology of the ultimate self-assembled superstructure. By FDTD simulations, the vortices present hierarchical, nanoscale focusing effect and are responsive to illumination of different circular polarized lights, which may make them useful in future photothermal or optical components. The field intensity of the vortices can be enhanced by surface plasmon of GNRs, and can be increased with an increase in the superlattices size. This is beneficial to realize the applications based on the vortical superlattices.

This work is supported by NSFC (No. 61006078 and 11374069), National Basic Research Priorities Program of China (No. 2010CB934102), and the "Strategic Priority Research Program" of the Chinese Academy of Sciences, Grant No. XDA09020300.

Notes and references

[a] Laboratory for Nanodevices, National Center for Nanoscience and Technology, Beijing, 100190, China. E-mail: liuq@nanoctr.cn

[b] CAS Key Laboratory of Standardization and Measurement for Nanotechnology, Beijing, 100190, China.

[c] Laboratory for Biological Effects of Nanomaterials and Nanosafety, National Center for Nanoscience and Technology, Beijing, 100190, China.

[d] University of Chinese Academy of Sciences, Beijing, 100191, China.

1 Y. Min, M. Akbulut, K. Kristiansen, Y. Golan and J. Israelachvili, *Nature Materials*, 2008, **7**, 527-538.

2 K. J. M. Bishop, C. E. Wilmer, S. Soh and B. A. Grzybowski, *Small*, 2009, **5**, 1600-1630.

3 P. J. Stang, *Journal of the American Chemical Society*, 2012, **134**, 11829-11830.

4 J. L. Baker, A. Widmer-Cooper, M. F. Toney, P. L. Geissler and A. P. Alivisatos, *Nano Letters*, 2010, **10**, 195-201.

5 Q. Liu, Y. Cui, D. Gandner, X. Li, S. He and I. Smalyukh, *Nano letter*, 2010, **10**, 1347-1353.

6 S. Umadevi, X. Feng and T. Hegmann, *Advanced Functional Materials*, 2013, **23**, 1393-1403.

7 Y. Xie, S. Guo, C. Guo, M. He, D. Chen, Y. Ji, Z. Chen, X. Wu, Q. Liu and S. Xie, *Langmuir*, 2013, **29**, 6232-6241.

8 H. Maeda, *Langmuir*, 1997, **13**, 4150-4161.

9 F. Kim, S. Kwan, J. Akana and P. Yang, *Journal of the American Chemical Society*, 2001, **123**, 4360-4361.

10 L.-s. Li, J. Walda, L. Manna and A. P. Alivisatos, *Nano Letters*, 2002, **2**, 557-560.

11 L. S. Li and A. P. Alivisatos, *Advanced Materials*, 2003, **15**, 408-411.

12 T. K. Sau and C. J. Murphy, *Langmuir*, 2005, **21**, 2923-2929.

13 R. Xu, H. Xin and B. Li, *Applied Physics Letters*, 2013, **103**, 014102-014105.

14 M. J. Hytch, R. E. Dunin-Borkowski, M. R. Scheinfein, J. Moulin, C. Duhamel, F. Mazaleyrat and Y. Champion, *Physical Review Letters*, 2003, **91**, 257207.

15 N. R. Jana, L. Gearheart and C. J. Murphy, *Advanced Materials*, 2001, **13**, 1389-1393.

16 Y. Xie, Y. Jia, Y. Liang, S. Guo, Y. Ji, X. Wu, Z. Chen and Q. Liu, *Chemical Communications*, 2012, **48**, 2128-2130.

17 T. Ming, X. Kou, H. Chen, T. Wang, H.-L. Tam, K.-W. Cheah, J.-Y. Chen and J. Wang, *Angewandte Chemie International Edition*, 2008, **47**, 9685-9690.

18 S. C. Warren, L. C. Messina, L. S. Slaughter, M. Kamperman, Q. Zhou, S. M. Gruner, F. J. DiSalvo and U. Wiesner, *Science*, 2008, **320**, 1748-1752.

19 A. Guerrero-Martinez, J. Perez-Juste, E. Carbo-Argibay, G. Tardajos and L. M. Liz-Marzan, *Angewandte Chemie International Edition*, 2009, **48**, 9484-9488.

20 W. Ahmed, E. S. Kooij, A. van Silfhout and B. Poelsema, *Nano Letters*, 2009, **9**, 3786-3794.

21 H. Hu and R. G. Larson, *Langmuir*, 2005, **21**, 3963-3971.

22 R. D. Deegan, O. Bakajin, T. F. Dupont, G. Huber, S. R. Nagel and T. A. Witten, *Nature*, 1997, **389**, 827-829.

23 W. Chen, D. C. Abeysinghe, R. L. Nelson and Q. Zhan, *Nano Letters*, 2009, **9**, 4320-4325.

24 S. Yang, W. Chen, R. L. Nelson and Q. Zhan, *Optics Letters*, 2009, **34**, 3047.

25 D. Giljohann, D. Seferos, W. Daniel, M. Massich, P. Patel and C. Mirkin, *Angewandte Chemie International Edition*, 2010, **49**, 3280-3294.

26 A. V. Kabashin, P. Evans, S. Pastkovsky, W. Hendren, G. A. Wurtz, R. Atkinson, R. Pollard, V. A. Podolskiy and A. V. Zayats, *Nature Materials*, 2009, **8**, 867-871.

27 X. Huang, S. Neretina and M. A. El-Sayed, *Advanced Materials*, 2009, **21**, 4880-4910.

28 Z. Zhu, H. Meng, W. Liu, X. Liu, J. Gong, X. Qiu, L. Jiang, D. Wang and Z. Tang, *Angewandte Chemie International Edition*, 2011, **50**, 1593-1596.

Nanoscale Accepted Manuscript

 This journal is © The Royal Society of Chemistry 2012

A table of contents entry

Vortical superlattices in gold nanorods self-assembly monolayer

Yong Xie[a], Yujia Liang[a, d], Dongxue Chen[a, d], Xiaochun Wu[b], Luru Dai[c] and Qian Liu*[a]

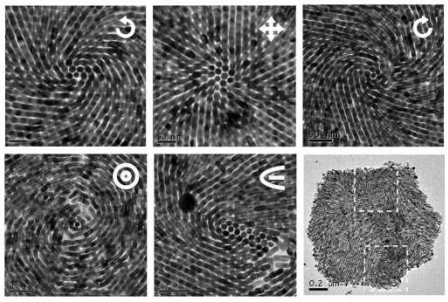

Various vortical superlattices of gold nanorods were obtained by a controlled droplet evaporation method, suggesting the possible manipulation of ultimate self-assembled superstructure by organic liquid crystal template or microfluidic droplet.

Nanoscale Accepted Manuscript